Experimental and numerical study on adhesion force in nanoscale

Su-Hyun Kim[1,2◆], Pan-Kyu Choi[1,2◆], Yong-Bok Lee[1], Tae-Soo Kim[1], Min-Seung Jo[1], So-Young Lee[1], Hyun-Woo Min[1,2] and Jun-Bo Yoon[1*]

[1] School of Electrical Engineering, Korea Advanced Institute of Science and Technology (KAIST), 291 Daehak-ro, Yuseong-gu, Daejeon 34141, Republic of Korea

[2] SAMSUNG ELECTRONICS Co., Ltd. 1, Samsungjeonja-ro, Hwaseong-si, Gyeonggi-do 18448, Republic of Korea

Corresponding author; Jun-Bo Yoon

Tel: +82-42-350-3476, Fax: +82-42-350-8565, E-mail: jbyoon@kaist.ac.kr

This file includes:

Supplementary Chapter S1-S6

Supplementary Figures 1 to 7, Tables 1, and Video 1

MATLAB Code for calculating adhesion force at Supplementary S6

Supplementary References

Table of Contents

Supplementary S1. Assumption of proposed model

For the proposed nanoscale contact model to imitate the realistic contact process of the rough surface, an appropriate assumption is needed that makes the analysis simple enough but does not cause a significant error. The proposed contact model adopted the following assumptions:

a) The rough surfaces exhibit isotropic and homogeneous characteristics.

b) The summits of all asperities take on a spherical shape.

c) The summits of all asperities share a uniform radius, denoted as R, while the heights of the asperities vary.

d) Deformation of the asperities on surfaces only occur during contact, with no bulk deformation of the mass body.

e) Interactions between asperities can be neglected

f) All contact processes are quasi-static.

g) The contact surfaces are contamination-free

h) Only dry adhesion is considered

i) The two contacting surfaces are of same material with identical work functions.

j) The two surfaces of contact are not hydrophilic.

Assumption a)-e) adopted the basic assumption of the Greenwood-Williamson (GW) model,[S1] which firstly analyzes the contact properties between rough surfaces based on asperities. McCool dealt with the anisotropic rough surface with the elliptical paraboloid asperities in his research[S2] and showed that the GW model's

assumption a)-c) is appropriate and sufficiently reflects contact conditions between surfaces. In assumption d), bulk deformation can be sufficiently ignored due to the stress distribution of larger bulk areas compared to contacting asperities. In addition, bulk deformation does not directly affect separation distance between asperities. Assumption e) implies that the proposed model independently analyzes the adhesions in each asperity. The total adhesions are calculated as the sum of the adhesions of all single asperities on the surfaces. Few previous models deal with coupled interaction of asperities on entire surfaces, but this approach is too complex to solve.[S3] So we focused on contact and adhesion analysis of uncoupled multi-asperities. Assumption f) assumes that the contact time until the adhesion force reaches the maximum value is long enough. Since the dynamic effects of elastic contact and plastic contact in the nanoscale are very small and negligible,[S4-5] we analyzed by simplifying the realistic contact process into a quasi-static process. Assumption g) can be the main cause of errors in the experiment, so it is essential to use enough clean surfaces as much as possible to achieve more accurate results. Assumption (h) clearly indicates that our contact model excludes the effect of capillary forces induced by humidity. To mitigate the impact of capillary forces and other potential effects related to humidity, all experiments presented in this paper were deliberately conducted at very low relative humidity levels (<25%).[S6] Should future research successfully incorporate the influence of capillary forces into the contact model, this assumption may be revisited. Furthermore, assumption (i) asserts that unintentional generation of electrostatic forces, resulting from an imbalance of electrons or ions, is not accounted for in our model because the contacting surfaces are made of the same material.[S7-8] However, if distinct voltages are intentionally applied to the contacting surfaces, any developed electrostatic force is considered an externally applied force. Lastly, assumption (j) signifies the exclusion of the impact of hydrogen bonding arising from hydrophilic surfaces.[S9-11]

Supplementary S2. Surface modeling based on AFM roughness data

The unique feature of a rough surface is that the roughness of the surface has a fractal structure, as shown in Figure S1(a).[S12-14] This 'Scale-independent' surface roughness consists of multi-asperities. The asperities on real rough surfaces vary in size and are non-uniformly distributed. This model assumes the pixel size of the AFM roughness data to be the diameter of the asperities and all of the asperities on the top and bottom surfaces to be aligned (Figure S1(b)).

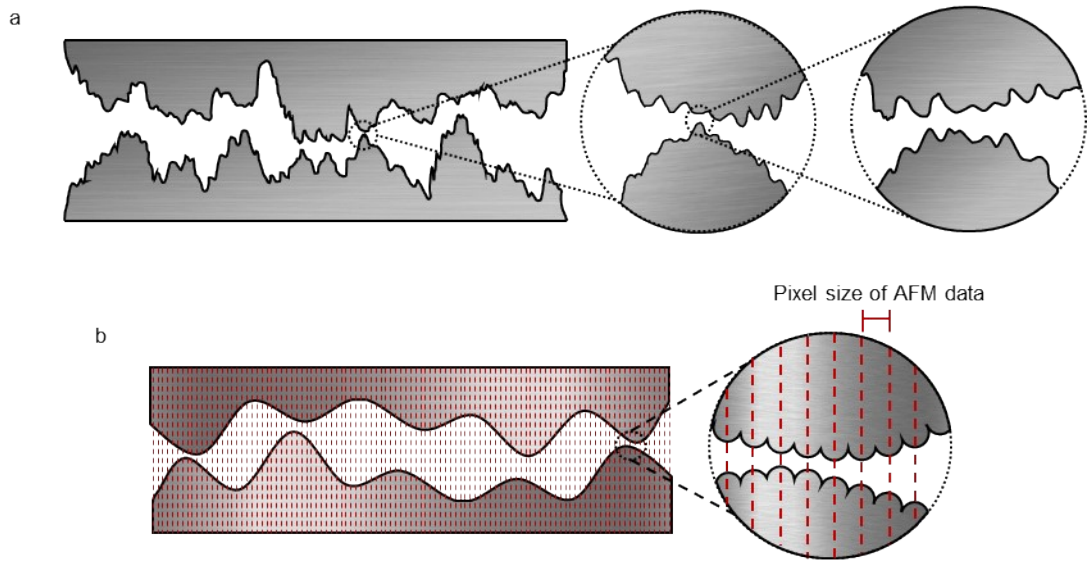

Figure S1. Real rough surface and modeling of the rough surface using AFM roughness data. a, Multiscale level of asperities on real rough surfaces. It shows fractal structure. b, Multi-asperities modeled by assumptions using AFM roughness data. The diameter of asperities is the pixel size of AFM data.

Supplementary S3. Analysis of nanoscale contact properties between surfaces

Videos S1. Visualization of nanoscale contact process between two contacting surfaces. Visual demonstration of our analysis showing dynamically changing contact between asperities and the physical gap between contact interfaces until final equilibrium separation distance is reached. The 3-dimensional visualization shows the exact location of the initial contact point between interfaces and enables precise calculation of the magnitude of deformation between individual asperities in contact.

Supplementary S4. Experimental Verification with AFM experiments

1) AFM F-d measurement

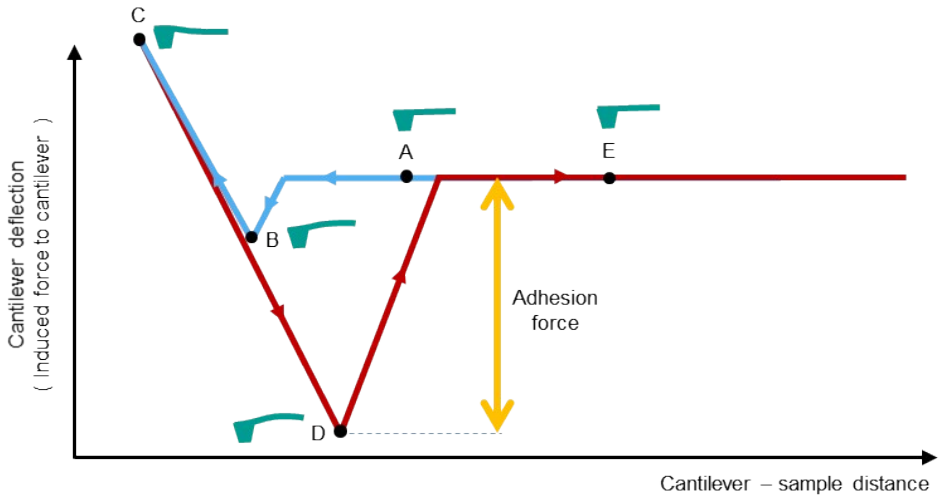

Fig S2. F-d curve of AFM measurement The Image shows an exemplary F-d curve with five types of regions labeled with the letters A to E (Blue solid line: tip approach, red solid line: tip retraction).[S15] Region A is no measurable tip-sample interaction because the tip is far from the surface. In region B, jump-into-contact is caused by attractive forces between tip and sample. The jump-into-contact occurs when the attractive force exceeds the restoring force of the cantilever. As the Z scanner of the AFM continues to descend toward the sample surface, the repulsive force continues to increase and reaches a predetermined force. In this case, the setpoint at which the Z scanner retracts the tip from the sample surface is region C. The cantilever is bent toward the sample surface in region D due to adhesion. Finally, in region E, the cantilever detaches from the surface when the restoring force of the cantilever overcomes the adhesion force between the tip and sample. In this curve, the adhesion force can be measured from the maximum negative value in the retraction curve.

2) Surface roughness measurement of the sample and the AFM probe.

The pixel size of the surface roughness data was measured to be 7.2 nm. The surfaces of the tip and the sample are consistent, so we measured part of the surface on the tip and the sample randomly. The exact location of the contact between the tip and the sample is not known when they are in contact, so we predicted adhesion force by drawing results from various combinations of top and bottom surfaces. For this reason, the predicted values in some of the graphs include error bars.

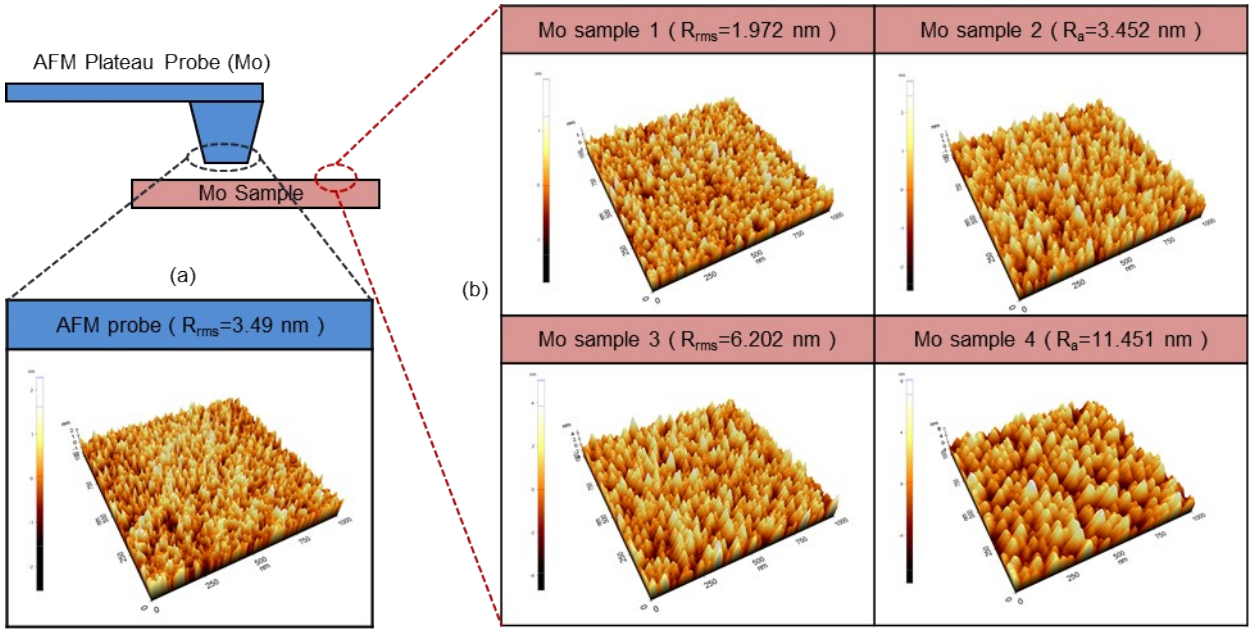

Fig S3. AFM image of plateau probe and sample tip for Mo-Mo(metallic) contact experiment. a, Surface roughness image of AFM plateau probe which is coated by molybdenum 30 nm. The RMS roughness of the plateau probe surface is 3.49nm. **b,** Surface roughness image of molybdenum sample. The samples were prepared to have varying roughness values, which were carefully controlled by depositing disparate thickness

of molybdenum. The RMS roughness values of each samples with 30nm, 50nm, 100nm, and 300nm of molybdenum sputtered on Si substrate were measured to be 1.972nm, 3.452nm, 6.202nm, and 11.451nm, respectively.

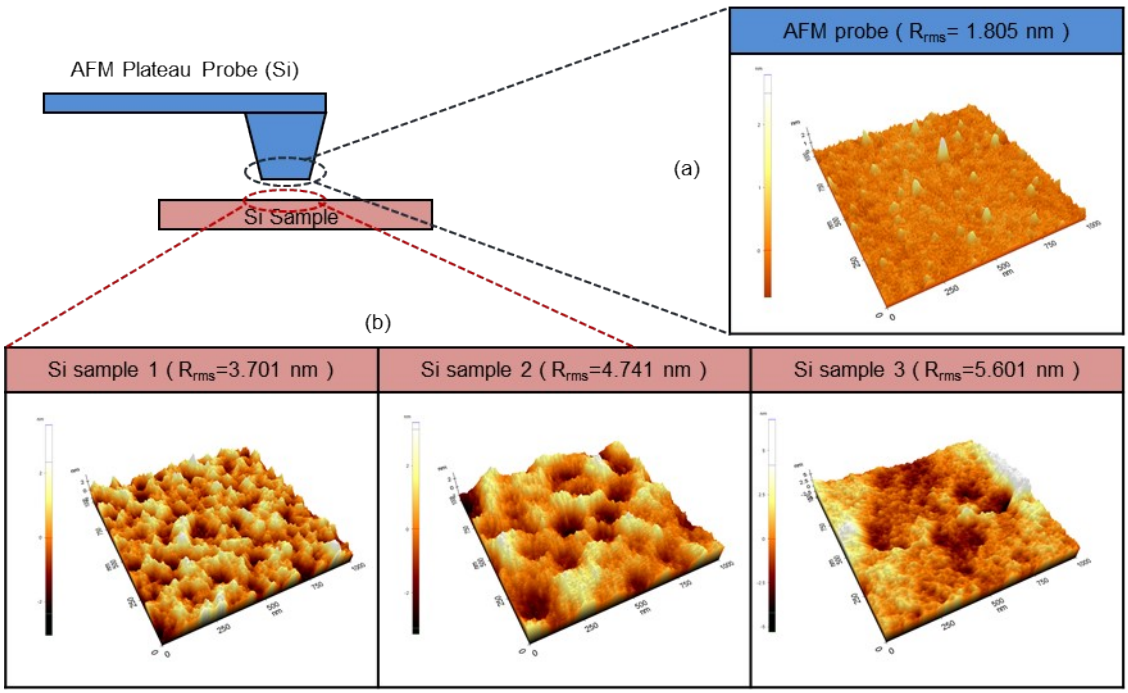

Fig S4. AFM image of plateau probe and sample tip for Si-Si(non-metallic) contact experiment. a, Surface roughness image of AFM plateau probe made by silicon. The RMS roughness of the plateau probe surface is 1.805nm. **b,** Surface roughness image of silicon sample. The RMS roughness of each sample was measured to be 3.701 nm, 4.741 nm, and 5.601 nm respectively. The roughness of the samples was split by controlling the etching condition. The roughness values increased with higher KOH concentration. The etching conditions using KOH were as follows: (1) KOH 0.4 vol% with 150ml of IPA for 2 minutes at 65C, (2) KOH 2 vol% with 150ml of IPA for 2 minutes at 65C, and (3) pure KOH with with 150ml of IPA for 2 minutes at 65C.

3) Material properties of molybdenum and silicon

When analyzing the contact between the two contacting surfaces using the proposed model, the contact property and adhesion force were calculated using values of the material property in Table S1. Other properties referred to the reference, but in the case of hardness, the deviation between references was large, so we measured the hardness using nano-indentation (Fig.S5).

Material property	Mo	Si
Surface energy (γ) [J/m]	3 [S16]	1.4 [S21]
Young's modulus (E) [GPa]	340 [S17]	179 [S17]
Hamaker constant (A) [J]	4.81×10^{-19} [S18]	2×10^{-19} [S21]
Intermolecular distance (ε) [nm]	0.272 [S19]	0.234 [S19]
Poisson's ratio (ν)	0.29 [S20]	0.27 [S17]
Hardness [GPa]	7.5	12.94

Table S1. Material properties of Molybdenum and silicon

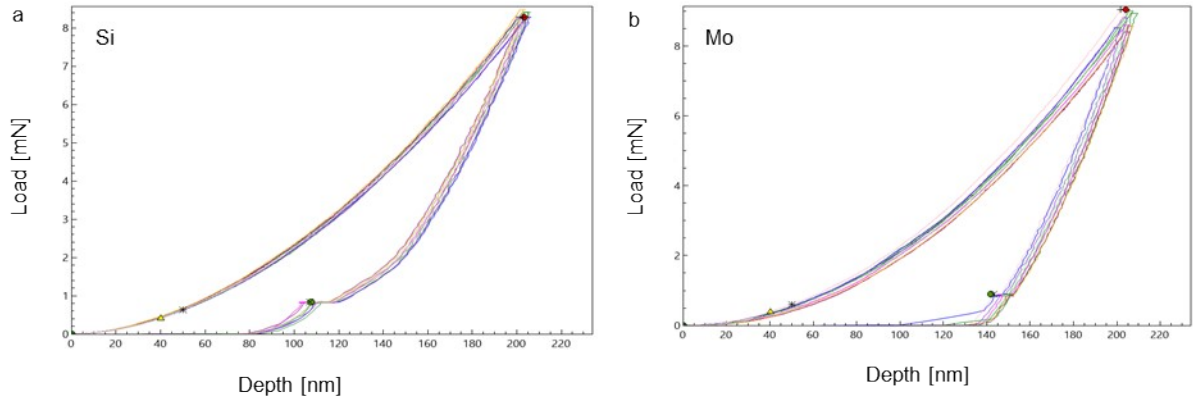

Figure S5. Nano-indentation curve for obtaining hardness. The average value measured 9 times through the experiment was used. **a,** The average hardness of silicon is 12.94 GPa and standard deviation is 0.516 GPa. **a,** The average hardness of molybdenum is 7.586 GPa and standard deviation is 1.195 GPa.

Supplementary S5. Verification of the nanoscale contact model using nano-switching device

We fabricated a Mo-contacting NEMS device for verifying that the proposed model can predict contact properties in addition to the adhesion force through electrical contact resistance comparison. Since the electrical contact resistance in nanoscale is greatly influenced by the real contact area, like the adhesion force, it is important to accurately predict the real contact area of the contacting asperities at the final separation distance. Until now, however, there has been no exact way to obtain nanoscale's electrical contact resistance, as there has been no way to predict a real contact area between the two surfaces in contact. Most previous studies have calculated the contact radius using Wexler equation (Equation1)[S22], assuming total contact radius of the several contacting asperities is same with the contact radius of single effective contacting asperities. And the contact radius of single effective contacting asperities can be calculated using equation 2 or equation 3.[S23-25] The proposed model allows more accurate analysis because it is possible to predict the contact radius of the individual contacting asperities. Therefore, we use a method to obtain the total electrical contact resistance by calculating the electrical contact resistance in individual contacting asperities by obtaining the sum of parallel resistances by obtaining the individual contact radius of contact in the final separation distance. Therefore, we use the proposed model to obtain the contact radius of the individual contacting asperities,

calculate the electrical contact resistance in the individual contacting asperities, and obtain the sum of the parallel resistances.

$$R_c = R_{wexler} = f\left(\frac{\lambda}{a}\right)R_O + R_S = \frac{1 + 0.88(\frac{\lambda}{a})}{1 + 1.33(\frac{\lambda}{a})}\frac{\rho}{2a} + \frac{4\rho\lambda}{3\pi a^2} \cdots\cdots\cdots\cdots\cdots\cdots Equation(1)$$

(R_c : Electron contact resistance ρ : Electrical resistivity a : Contact radius λ : Electron mean free path)

$$a = \sqrt{\frac{F}{\pi H}}(Plastic\ deformation) \cdots\cdots\cdots\cdots\cdots\cdots\cdots\cdots Equation(2)$$

$$a = \sqrt{\frac{3FR}{4E^*}}(Elastic\ deformation) \cdots\cdots\cdots\cdots\cdots\cdots\cdots\cdots Equation(3)$$

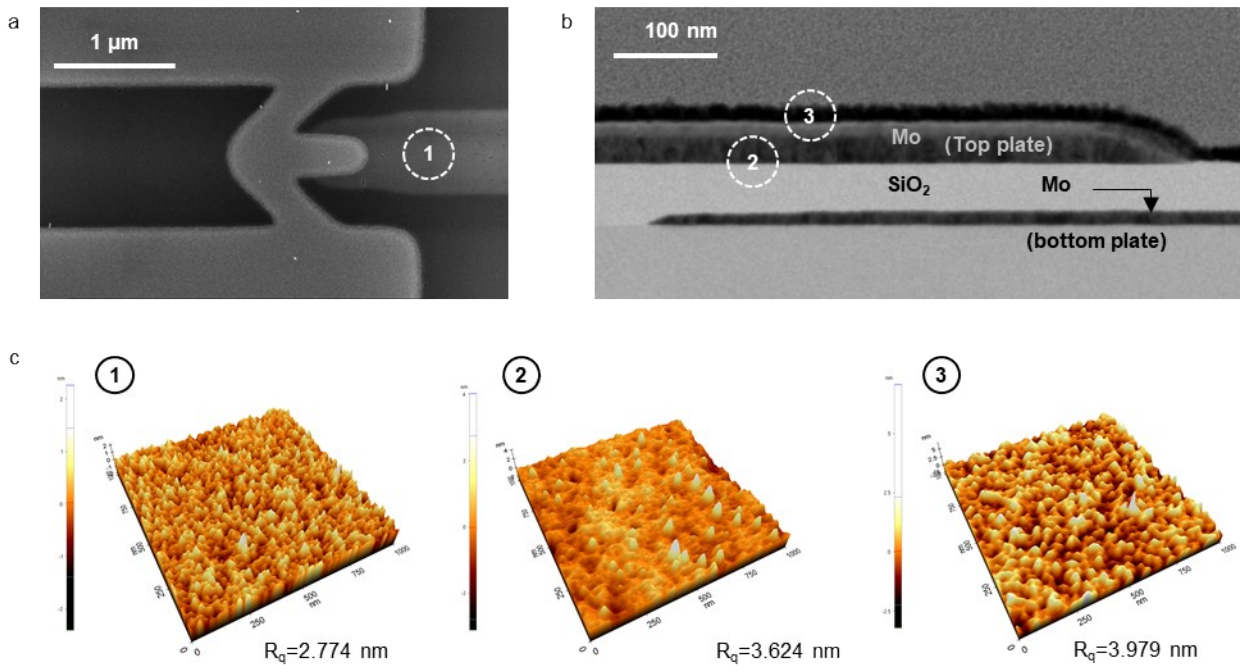

Fig S6. Images of Mo-contacting NEMS switching device. a, Top view of device (SEM image). The thickness of top plate is about 38nm. **b,** Side view of device (TEM image). The thickness of bottom plate is about 12nm and that of silicon oxide is 42nm. **c,** AFM image of top and bottom surface of NEMS switching

device.

Prior to applying the proposed model, the surface of the element manufactured to obtain the surface information of the element we want to analyze was measured with AFM. The bottom electrode of NEMS switching device can be easily measured by AFM. However, the lower part of top electrode is difficult to measure because we cannot turn top electrode which has nano-size thickness inside out. Accordingly, we measured the upper part of SiO2(②)and the upper part of top Mo(③) which are expected to have similar morphology with the lower part of top electrode due to print-through effect from the deposition process of the nanoscale.[S26]

The result of the comparison between the measured value of the NEMS device and the predicted value of the proposed model is shown in Figure S9. The calculated electrical contact resistance showed an error of 9.5% compared to the measured value of the NEMS device. This is a sufficiently accurate value considering various factors such as measurement error of NEMS switching device and surface roughness measurement error. This result shows that the proposed model will serve as the basis for predicting various contact properties.

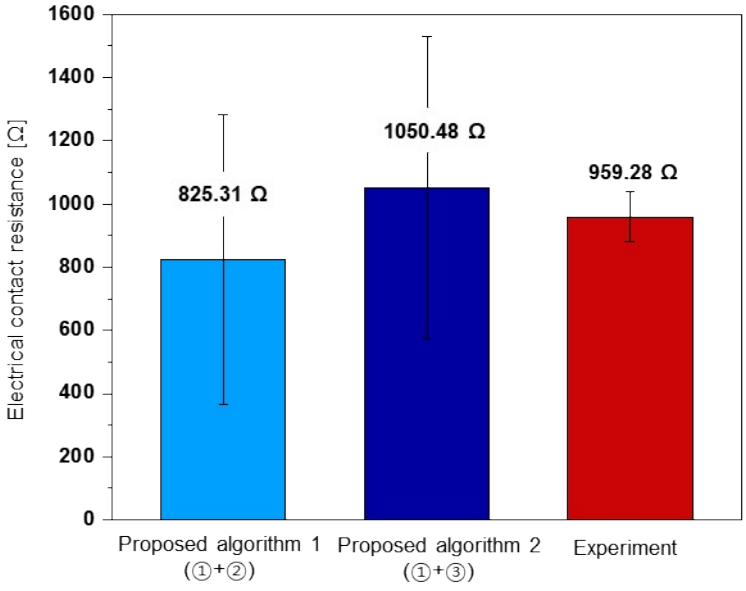

Fig S7. Comparison of electrical contact resistance between proposed model and measurement results. Model 1 used roughness data obtained from SiO_2 top surface and Mo bottom surface. Model 2 used roughness data obtained from Mo top surface and Mo bottom surface.

Supplementary S6. MATLAB code for utilizing proposed model

```
% Created by Su-hyun Kim & Pan-Kyu Choi
% Title: Adhesion Force Calculation

% *** User Guideline ***
% 0. Put this code in MATLAB and keep it aside
% 1. Modify the filename of excel, sheet name, and the range of the AFM surface roughness data
% 2. Modify to the properties of the material and condition of contact which you want to predict
% 3. Run this code

% Main result
% 1) F_adhesion_final : Final adhesion force
% 2) avg_sep_ini / avg_sep_final : initial and final average separation distance



%% Upload AFM roughness data of Top surface (need to check before run the code)

% Excel and matlab files must be in the same folder.
% Upper and lower case sensitive

Top_data_1 = xlsread('filename.xlsx', 'Sheet1', 'C8:C65543');  % Put the filename of excel, sheet name, and the range of the data
% Top_data_2 = xlsread('filename,xlsx', 'Sheetname', 'Range'); % If multiple files or sheets or ranges are used, add according to the format provided.

Top_tot=Top_data_1; % Create data set suitable for the area you want to analyze.
% Top_tot=[Top_data_1;Top_data_2;Top_data_3]; or Top_tot=[Top_data_1;Top_data_1]; % Example of multiple data set



%% Upload AFM roughness data of Bottom surface (need to check before run the code)

Bottom_data_1 = xlsread('filename.xlsx', 'Sheet1', 'C8:C65543');  % Put the filename of excel, sheet name, and the range of the data
```

```
% Bottom_data_2 = xlsread('filename,xlsx', 'Sheetname', 'Range'); % If multiple files or sheets or ranges are used, add according to the format provided.

Bottom_tot=Bottom_data_1; % Create data set suitable for the area you want to analyze.
% Bottom_tot=[Bottom_data_1;Bottom_data_2; Bottom_data_3]; or
Bottom_tot=[Bottom_data_1;Bottom_data_1]; % Example of multiple data set



%% Randomize the surface roughness data

% Predict adhesion force by drawing results from various combinations of top and bottom surfaces because the exact location of the contact between the tip and the sample is not known when they are in contact

Top=Top_tot;
%Top_random1=Top(randperm(length(Top)));
%Top_random2=Top(randperm(length(Top)));
%Top_random3=Top(randperm(length(Top)));

Bottom=Bottom_tot;
%Bottom_random1=Bottom(randperm(length(Bottom)));
%Bottom_random2=Bottom(randperm(length(Bottom)));
%Bottom_random3=Bottom(randperm(length(Bottom)));



%% Properties of material (need to check and modify before run the code)
% This is an example of molybdenum.
E=340*10^9; % Young's modulus [Pa]
v=0.29; % Poisson ratio
surfE=3;% Surface energy [J/m^(-2)]
H=4.81*10^(-19); % Hamaker Constant [J]
Hardness=7.5*10^9; % Hardness [Pa]
intermo_d=0.136*2*10^(-9); % Intermolecular distance [m]
```

```
%% Condition of contact (need to check and modify before run the code)

Pixel = 7.8124; % Pixel size of measured AFM data (Diameter of Asperity) [nm]
Apparent_area = 44*10^(-12) ; %  Total apparent area of contact [m^2]
F_ext=100*10^(-9); % Applied external force [N]


%% Set bottom & top surfaces (need to check and modify before run the code)

A = (Bottom_tot+Top_tot); % Input the top and bottom surface to use (Total height of top and bottom asperities)
% A = (Bottom_random1+Top_random1); % Use this statement if you want to input various combinations of surface.


%% Extra parameter calcultation

% Pixel area of roughness data
Pixel_area = (Pixel*10^(-9))^2;

% Radius of curvature of asperity
r1=0.5*(Pixel)*10^(-9);
r2=0.5*(Pixel)*10^(-9);
R_particle=((r1*r2)/(r1+r2)); % Effective radius of curvature

% Elastic constant of the material
k1=(1-v^2)/E;
k2=(1-v^2)/E;
E_eff=1/(k1+k2); % Effective elastic modulus
K_particle=4/(3*(k1+k2));
```

```
% Work of adhesion
Work_adh=2*surfE;

% Parameter of correction function of van der waals force
b=3.1;
wl=100*10^-9;  % Wave length
c=b*wl/(2*pi);

% Critical parameter
H_coeff=0.454+0.41*v; % Hardness coefficent
indent_c=(((pi*H_coeff*Hardness)/(2*E_eff))^2)*r1; % Critical indentation
force_c=(2/3)*H_coeff*Hardness*pi*indent_c*r1; % Critical contact force

% Tabor parameter
Tabor_p=((R_particle*(Work_adh)^2)/(((E_eff)^2)*((intermo_d)^2)))^(1/3);


%% Save the information in each step of iteration process

Adh_vdW_array=[]; % Adhesion force from non-contacting asperities (Van der Waals force)
Adh_Asp_array=[]; % Adhesion force from contacting asperity
Adh_Force_array=[]; % Total Adhesion force
Adh_avgsep_array=[]; % Average separation distance between surfaces
Adh_Delta_array=[]; % Distance to next contact
Contact_asp_num_array=[]; % Number of contacting asperities
E_asp_num_array=[]; % Number of asperities in elastic deformation region
EP1_asp_num_array=[]; % Number of asperities in first elastic-plastic deformation region
EP2_asp_num_array=[]; % Number of asperities in second elastic-plastic deformation region
P_asp_num_array=[]; % Number of asperities in plastic deformation region


%% Modeling of bottom & top surfaces
```

```
A_sorted=sort(A,'descend'); % Height from highest to lowest
height = max(A_sorted); % First contacting point
height_ini = height; % Height of first contacting asperity


%% Analyze first contacting asperities (Loading)

index = find(A==height); % Find the real contacting asperities
Delta=height-A_sorted(1+length(index)); % Distance to next contact

% Separation distance Analysis
d_sep = [zeros(length(index),1); height - A_sorted((1+length(index)):length(A_sorted))]; % Separation
distance of non-contacting asperities based on height of first contacting asperities
avg_sep = mean(d_sep); % Initial average separation distance
avg_sep_ini=avg_sep; % Save the information of initial average separation distance
D_sep=(avg_sep+0.165)*10^-9; % Add cutoff separation distance

% Adhesion force analysis of non-contacting region : Van der Waals Adhesion Force Calculation
g=1-(2*D_sep/c)+(6*(D_sep.^2)./c^2)+((12*D_sep.^3)./c^3)-
((12*D_sep.^3)./c^4).*(D_sep+c).*log(1+c./D_sep); % Correction function
F_adh_VdW_unit_area=(H./(6*pi.*D_sep.^3)).*g;
F_adh_VdW = F_adh_VdW_unit_area * (Apparent_area-Pixel_area*length(index));

% Adhesion force analysis of contacting region : Elastic deformation region
if Tabor_p<1
   F_asperity_adh_contact= 2*pi*R_particle*Work_adh; % DMT theory
else
   F_asperity_adh_contact= (3/2)*pi*R_particle*Work_adh; % JKR theory
end

% Total applied force between surfaces (External force + Adhesion force)
F_asperity_applied=(F_ext+F_adh_VdW)/length(index)+F_asperity_adh_contact;
```

```
% Contact analysis of each deformation region

if F_asperity_applied<=force_c % Elastic deformation region
   if Tabor_p<1
      contact_radius=(F_asperity_applied*r1/K_particle)^(1/3); % DMT theory
      indent= (contact_radius)^2/r1; % DMT theory

   else

contact_radius=(r1/K_particle)*(F_asperity_applied+3*pi*Work_adh*r1)+(6*pi*Work_adh*r1*F_asperit
y_applied+(3*pi*Work_adh*r1)^2)^(1/2); % JKR theory
      indent= (contact_radius)^2/r1-((8*pi*contact_radius*Work_adh)/(3*K_particle))^(1/2); % JKR
theory
   end

elseif force_c<F_asperity_applied && F_asperity_applied<=force_c*1.03*(6^1.425) % Elastic-Plastic
deformation region 1
   indent=indent_c*(F_asperity_applied/(force_c*1.03))^(1/1.425);

elseif force_c*1.03*(6^1.425)<F_asperity_applied && F_asperity_applied<=force_c*1.4*(110^1.263) %
Elastic-Plastic deformation region 2
   indent=indent_c*(F_asperity_applied/(force_c*1.4))^(1/1.263);

else % Plastic deformation region
   indent=2*(F_asperity_applied/(pi*2*r1*Hardness));

end

%Save the information of first step of iteration process
Adh_vdW_array=[Adh_vdW_array,F_adh_VdW];
Adh_Asp_array=[Adh_Asp_array,F_asperity_adh_contact*length(index)];
Adh_Force_array=[Adh_Force_array,F_adh_VdW+F_asperity_adh_contact*length(index)];
Adh_avgsep_array=[Adh_avgsep_array,avg_sep];
```

```
Adh_Delta_array=[Adh_Delta_array,Delta];
Contact_asp_num_array=[Contact_asp_num_array,length(index)];
E_asp_num_array=[E_asp_num_array,length(index)];
EP1_asp_num_array=[EP1_asp_num_array,0];
EP2_asp_num_array=[EP2_asp_num_array,0];
P_asp_num_array=[P_asp_num_array,0];



%% Analyze n-th contacting asperities (Loading)

num = length(index); % for-loop initial parameter

while num<length(A_sorted)+1 % Finish the process when all the asperities are analyzed
   if indent >= (abs( height_ini - A_sorted(num+1) ))*10^-9 % Comparison between separation distance between the asperities and deformation of the first asperity pair

      height = A_sorted( num+1 ); % Height of n-th contacting asperity
      index = find(A==height); % Find the index of the aspertiy
      num = length(index) + num; % Find the total number of contacting asperities

      Delta=height-A_sorted(1+num); % Distance to next contact

      % Separation distance Anlysis
      d_sep = [zeros(num,1); height - A_sorted((1+num):length(A_sorted))]; % Separation distance of non-contacting asperities based on height of n-th contacting asperities
      avg_sep = mean(d_sep); % Initial average separation distance
      D_sep=(avg_sep+0.165)*10^-9; % Add cutoff separation distance



      %% Adhesion force analysis of n-th contacting asperities (Loading)

      % Adhesion force analysis of non-contacting region : Van der Waals Adhesion Force Calculation
      g=1-(2*D_sep/c)+(6*(D_sep.^2)./c^2)+((12*D_sep.^3)./c^3)-
```

```
((12*D_sep.^3)./c^4).*(D_sep+c).*log(1+c./D_sep); %correction function
    F_adh_VdW_unit_area=(H./(6*pi.*D_sep.^3)).*g;
    F_adh_VdW = F_adh_VdW_unit_area * (Apparent_area-Pixel_area*num);

    % Distinguish the deformation range of contacting asperities
    indent_array=(A_sorted(1:num)-height)*10^(-9); % Deformation array of contacting asperities
    E_contact=indent_array(indent_array<=indent_c); % Contacting asperities in elastic deformation region
    EP1_contact=indent_array(indent_c<indent_array & indent_array<=6*indent_c); % Contacting asperities in elastic-plastic deformation region 1
    EP2_contact=indent_array(6*indent_c<indent_array & indent_array<=110*indent_c); % Contacting asperities in elastic-plastic deformation region 2
    P_contact=indent_array(110*indent_c<indent_array); % Contacting asperities in plastic deformation region

    % Adhesion force analysis of contacting region : Elastic deformation region
    E_adhesion=F_asperity_adh_contact*length(E_contact);

    % Adhesion force analysis of contacting region : Elastic-plastic deformation region
    if 0.005<=intermo_d/indent_c && intermo_d/indent_c<=0.5
        EP1_adhesion=(0.792.*(intermo_d./indent_c).^(-0.321).*(EP1_contact./indent_c).^(0.356))*F_asperity_adh_contact;
        EP2_adhesion=(1.193.*(intermo_d./indent_c).^(-0.332).*(EP2_contact./indent_c).^(0.093))*F_asperity_adh_contact;

    elseif 0.5<intermo_d/indent_c && intermo_d/indent_c<=100

EP1_adhesion=(0.961+0.157/(intermo_d/indent_c)+0.261.*log(EP1_contact./indent_c)./(intermo_d./indent_c))*F_asperity_adh_contact;
        EP2_adhesion=(1.756-(0.516-0.303./(intermo_d./indent_c)).*log(EP2_contact./indent_c)+0.052.*(log(EP2_contact./indent_c)).^2)*F_asperity_adh_contact;
```

```
    end

    % Adhesion force analysis of contacting region : Plastic deformation region
    P_adhesion=pi*2*R_particle*Hardness*P_contact;

    % Total adhesion force
    F_adhesion=E_adhesion+sum(EP1_adhesion)+sum(EP2_adhesion)+sum(P_adhesion)+F_adh_VdW;

    % Save the information
    Adh_vdW_array=[Adh_vdW_array,F_adh_VdW];

Adh_Asp_array=[Adh_Asp_array,E_adhesion+sum(EP1_adhesion)+sum(EP2_adhesion)+sum(P_adhesio
n)];
    Adh_Force_array=[Adh_Force_array,F_adhesion];
    Adh_avgsep_array=[Adh_avgsep_array,avg_sep];
    Adh_Delta_array=[Adh_Delta_array,Delta];
    Contact_asp_num_array=[Contact_asp_num_array,num];
    E_asp_num_array=[E_asp_num_array,length(E_contact)];
    EP1_asp_num_array=[EP1_asp_num_array,length(EP1_contact)];
    EP2_asp_num_array=[EP2_asp_num_array,length(EP2_contact)];
    P_asp_num_array=[P_asp_num_array,length(P_contact)];


%% contact analysis of n-th contacting asperities (Loading)

    % Total applied force between surfaces (External force + Adhesion force)
    F_asperity_applied=(F_ext+F_adh_VdW)/num+F_asperity_adh_contact;

    % Contact analysis of each deformation region
    if F_asperity_applied<=force_c   % Elastic deformation region
      if Tabor_p<1
        contact_radius=(F_asperity_applied*r1/K_particle)^(1/3); % DMT theory
        indent= (contact_radius)^2/r1; % DMT theory
```

```
        else

contact_radius=(r1/K_particle)*(F_asperity_applied+3*pi*Work_adh*r1)+(6*pi*Work_adh*r1*F_asperit
y_applied+(3*pi*Work_adh*r1)^2)^(1/2); % JKR theory
            indent= (contact_radius)^2/r1-((8*pi*contact_radius*Work_adh)/(3*K_particle))^(1/2); % JKR
theory
        end

    elseif force_c<F_asperity_applied && F_asperity_applied<=force_c*1.03*(6^1.425) % Elastic-
Plastic deformation region 1
        indent=indent_c*(F_asperity_applied/(force_c*1.03))^(1/1.425);

    elseif force_c*1.03*(6^1.425)<F_asperity_applied &&
F_asperity_applied<=force_c*1.4*(110^1.263) % Elastic-Plastic deformation region 2
        indent=indent_c*(F_asperity_applied/(force_c*1.4))^(1/1.263);

    else % Plastic deformation region
        indent=2*(F_asperity_applied/(pi*2*r1*Hardness));

    end


  else

    % Decide final separation distance
    if indent <= (abs( height_ini - A_sorted(num) ))*10^-9
        height_final=A_sorted(num);
    elseif height_ini-indent*(10^9)+indent_c > A_sorted(num)
        height_final=A_sorted(num);
    else
        height_final=height_ini-indent*(10^9)+indent_c;
    end
```

```
d_sep = [zeros(num,1); height_final - A_sorted((1+num):length(A_sorted))]; % Separation distance of non-contacting asperities based on height of final contacting asperities
avg_sep = mean(d_sep); % Average separation distance
avg_sep_final=avg_sep;
D_sep=(avg_sep+0.165)*10^-9; % Add cutoff separation distance


% Adhesion force analysis of non-contacting region : Van der Waals Adhesion Force Calculation
g=1-(2*D_sep/c)+(6*(D_sep.^2)./c^2)+((12*D_sep.^3)./c^3)-((12*D_sep.^3)./c^4).*(D_sep+c).*log(1+c./D_sep); %correction function
F_adh_VdW_unit_area=(H./(6*pi.*D_sep.^3)).*g;
F_adh_VdW = F_adh_VdW_unit_area * (Apparent_area-Pixel_area*num);

% Distinguish the deformation range of contacting asperities
indent_array=(A_sorted(1:num)-height_final)*10^(-9); % Deformation array of contacting asperities
E_contact=indent_array(indent_array<=indent_c); % Contacting asperities in elastic deformation region
EP1_contact=indent_array(indent_c<indent_array & indent_array<=6*indent_c); % Contacting asperities in elastic-plastic deformation region 1
EP2_contact=indent_array(6*indent_c<indent_array & indent_array<=110*indent_c); % Contacting asperities in elastic-plastic deformation region 2
P_contact=indent_array(110*indent_c<indent_array); % Contacting asperities in plastic deformation region

% Adhesion force analysis of contacting region : Elastic deformation region
E_adhesion=F_asperity_adh_contact*length(E_contact);

% Adhesion force analysis of contacting region : Elastic-plastic deformation region
if 0.005<=intermo_d/indent_c && intermo_d/indent_c<=0.5
    EP1_adhesion=(0.792.*(intermo_d./indent_c).^(-0.321).*(EP1_contact./indent_c).^(0.356))*F_asperity_adh_contact;
    EP2_adhesion=(1.193.*(intermo_d./indent_c).^(-0.332).*(EP2_contact./indent_c).^(0.093))*F_asperity_adh_contact;
```

```
    elseif 0.5<intermo_d/indent_c && intermo_d/indent_c<=100

EP1_adhesion=(0.961+0.157/(intermo_d/indent_c)+0.261.*log(EP1_contact./indent_c)./(intermo_d./indent_c))*F_asperity_adh_contact;
        EP2_adhesion=(1.756-(0.516-0.303./(intermo_d./indent_c)).*log(EP2_contact./indent_c)+0.052.*(log(EP2_contact./indent_c)).^2)*F_asperity_adh_contact;

    end

    %Adhesion force analysis of contacting region : Plastic deformation region
    P_adhesion=pi*2*R_particle*Hardness*P_contact;

    % Final adhesion force force
    F_adhesion=E_adhesion+sum(EP1_adhesion)+sum(EP2_adhesion)+sum(P_adhesion)+F_adh_VdW;
    F_adhesion_final=F_adhesion;

    %Save the information
    Adh_vdW_array=[Adh_vdW_array,F_adh_VdW];

Adh_Asp_array=[Adh_Asp_array,E_adhesion+sum(EP1_adhesion)+sum(EP2_adhesion)+sum(P_adhesion)];
    Adh_Force_array=[Adh_Force_array,F_adhesion];
    Adh_avgsep_array=[Adh_avgsep_array,avg_sep];
    E_asp_num_array=[E_asp_num_array,length(E_contact)];
    EP1_asp_num_array=[EP1_asp_num_array,length(EP1_contact)];
    EP2_asp_num_array=[EP2_asp_num_array,length(EP2_contact)];
    P_asp_num_array=[P_asp_num_array,length(P_contact)];

    % Additional information
    plastic_ratio=length(P_contact)/num; % Percentage of asperities in plastic deformation range
```

```
        break
    end
end

fprintf('The final adhesion force is %d [N].\n',F_adhesion_final)
```

Reference

[S1] J. A. Greenwood and J. P. Williamson, *Proceedings of the royal society of London. Series A. Mathematical and physical sciences*, 1966, **295**, 300-319.

[S2] J. I. McCool, *Journal of Tribology*, 1986, **108**, 380-385.

[S3] P. Prokopovich and V. Starov, *Advances in colloid and interface science*, 2011, **168**, 210-222.

[S4] M. Pashley, J. Pethica and D. Tabor, *Wear*, 1984, **100**, 7-31.

[S5] A. Thölén, *physica status solidi (a)*, 1980, **60**, 153-166.

[S6] F. P. Bowden and D. Tabor, *The friction and lubrication of solids*, Oxford university press, 2001.

[S7] R. Maboudian and R. T. Howe, *Journal of Vacuum Science & Technology B: Microelectronics and Nanometer Structures Processing, Measurement, and Phenomena*, 1997, **15**, 1-20.

[S8] H. Izadi, A. Zandieh and A. Penlidis, *Kirk-Othmer Encyclopedia of Chemical Technology*, 2000, 1-35.

[S9] E. Arunan, G. R. Desiraju, R. A. Klein, J. Sadlej, S. Scheiner, I. Alkorta, D. C. Clary, R. H. Crabtree, J. J. Dannenberg and P. Hobza, *Pure and applied chemistry*, 2011, **83**, 1637-1641.

[S10] R. Legtenberg, H. A. Tilmans, J. Elders and M. Elwenspoek, *Sensors and actuators A: Physical*, 1994, **43**, 230-238.

[S11] G. B. Kaufman, *Journal of Chemical Education*, 1993, 70, 10, A279

[S12] A. Majumdar and C. Tien, *Wear*, 1990, **136**, 313-327.

[S13] A. Majumdar and B. Bhushan, *Journal of Tribology*, 1990, **112**, 205-216.

[S14] A. Majumdar and B. Bhushan, *Journal of Tribology*, 1991, **113**, 1-11.

[S15] B. Cappella and G. Dietler, *Surface science reports*, 1999, **34**, 1-104.

[S16] F. De Boer, R. Boom, W. Mattens, A. Miedema and A. Niessen, " Cohesion in Metals North-Holland.", 1988.

[S17] C.-J. Tsai, D. Y. Pui and B. Y. Liu, *Aerosol Science and Technology*, 1991, **15**, 239-255.

[S18] P. Tolias, *Surface Science*, 2020, **700**, 121652.

[S19] J. F. Shackelford, *Introduction to materials science for engineers*, Pearson Upper Saddle River, 2016.

[S20] https://www.azom.com/properties.aspx?ArticleID=616

[S21] J. N. Israelachvili, *Intermolecular and surface forces*, Academic press, 2011.

[S22] G. Wexler, *Proceedings of the Physical Society*, 1966, **89**, 927.

[S23] Y.-H. Song, D.-H. Choi, H.-H. Yang and J.-B. Yoon, *J. Microelectromech. Syst.*, 2011, **20**, 204-212.

[S24] H. Kwon, S.-S. Jang, Y.-H. Park, T.-S. Kim, Y.-D. Kim, H.-J. Nam and Y.-C. Joo, *Journal of Micromechanics and Microengineering*, 2008, **18**, 105010.

[S25] B. F. Toler, R. A. Coutu and J. W. McBride, *Journal of Micromechanics and Microengineering*, 2013, **23**, 103001.

[S26] F. W. DelRio, M. P. de Boer, J. A. Knapp, E. David Reedy Jr, P. J. Clews and M. L. Dunn, *Nature materials*, 2005, **4**, 629-634.